JOURNAL OF COLLOID AND INTERFACE SCIENCE **182,** 220–229 (1996)
ARTICLE NO. 0454

Isotherms of Dipalmitoylphosphatidylcholine (DPPC) Monolayers: Features Revealed and Features Obscured

K. J. KLOPFER AND T. K. VANDERLICK[1]

University of Pennsylvania, Department of Chemical Engineering, 220 South 33rd Street, Philadelphia, Pennsylvania 19104-6393

Received December 12, 1995; accepted March 28, 1996

Pressure–area isotherms of dipalmitoylphosphatidylcholine (DPPC) exhibit a two-phase region wherein domains of a liquid-condensed (LC) phase are dispersed in the less ordered liquid-expanded (LE) phase. Fluorescence microscopy has been used over the past years to visualize the shapes displayed by DPPC domains throughout the coexistence region; characteristic domain shapes include those resembling dimpled beans and S-like figures. In this paper we show that the types and distributions of domain shapes formed throughout the coexistence region depend sensitively on the rate of monolayer compression. Additionally, by comparing the relative proportion of LE and LC phases observed to that which is predicted by the isotherm, we find apparent violations of the lever rule. Most importantly, we find that if the monolayer is allowed to age in a state of two-phase coexistence for long times (approx. 12 h), the DPPC domains all become nearly circular. Finally, isotherms generated by compressing very slowly, or those generated at quick speeds but only after the film was left stagnant for a few hours, are markedly different from isotherms produced if the film was compressed within an hour after it was spread. One likely explanation for this behavior is the accumulation of air-borne impurities. © 1996 Academic Press, Inc.

Key Words: **compression speed; domain shapes; impurities.**

INTRODUCTION

The workhorse of insoluble monolayer investigations is the Langmuir trough, which is used to generate pressure–area isotherms. An isotherm is one of the most fundamental characteristics of a monolayer system, and the analysis and interpretation of isotherms provide an easy route to learn about the state of the monolayer. In this regard, the shapes of isotherms, often fraught with kinks and plateaus, are extremely valuable road maps for hunting down phase and ordering transitions experienced by the monomolecular film. Long ago, Stallberg-Stenhagen and Stenhagen (1) made the most of this opportunity to postulate the many phases of fatty acid monolayers, results more recently confirmed by several other researchers using isotherm analysis as well as other more direct techniques (2–5).

Valuable as they are, isotherms may display features that are difficult to interpret, or may even be featureless under conditions where interesting things are happening. For example, the nonhorizontal nature of the plateau exhibited in the isotherms of many lipid monolayers (corresponding to the liquid-expanded (LE)/liquid-condensed (LC) phase transition) has remained cause for debate for over 25 years. Thus additional techniques are often called upon to resolve or further probe the state of monolayer films. One technique that has unveiled many intriguing monolayer properties is fluorescence microscopy, which allows visualization of coexisting phases. Not only did use of this technique confirm the presence of two coexisting phases within the lipid LE/LC plateau regime (6, 7), but pictures revealed the formation of domains (of the LC phase) with fascinating morphologies (8, 9). Shapes and sizes of monolayer domains have since been shown to depend on many variables such as chirality of the molecules (10), temperature (11), and subphase pH (12). Domain growth and form have also been investigated by Brewster angle microscopy (13, 14), which obviates the need to add a fluorescent probe to the system. This technique has been especially useful for imaging intradomain textures (15, 16) as well as domain shapes. Theories of domain shapes have been developed which rationalize shapes in terms of a competition between line tension (favoring compact circular shapes) and electrostatic dipole effects (which favor extended shapes) (17–24).

One particular monolayer system that has received much attention over the years (especially in laboratories housed with fluorescence microscopes) is the phospholipid dipalmitoylphosphatidylcholine (DPPC). DPPC is prominent in the lipid bilayer making up the cell membrane and is also a major constituent of lung surfactant. One of the first systems visualized with fluorescence microscopy was, in fact, DPPC (7). Given the quantity of attention directed at this system, DPPC monolayers are considered to be relatively well characterized. In fact most newcomers to the field often choose to start by reproducing DPPC isotherms and viewing the ''characteristic'' DPPC shapes. Perusal of the literature leads to the following portrayal of DPPC domain nucleation and growth: As long as the film is compressed over ranges of

[1] To whom correspondence should be addressed.

0021-9797/96 $18.00

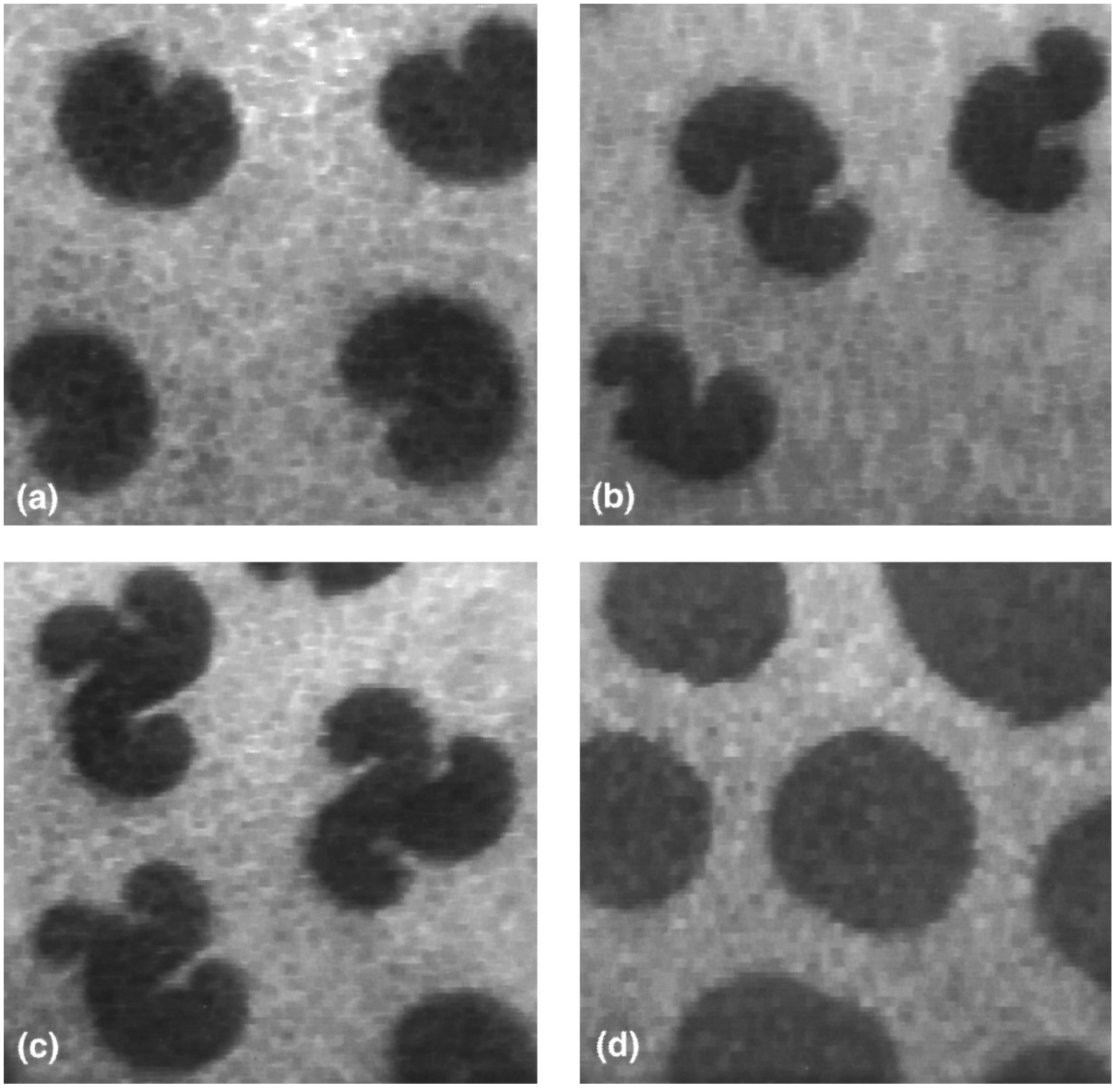

FIG. 1. Characteristic DPPC domain shapes: (a) beans (π = 3.8 mN/m, A = 72.7 Å^2/molecule); (b) S shapes (π = 3.9 mN/m, A = 69.5 Å^2/molecule); (c) multilobes (π = 4.1 mN/m, A = 53.5 Å^2/molecule); (d) circles (aged for 10 h, A = 53.5 Å^2/molecule). Scale, 1.5 cm = 27 μm.

speed that are generally considered slow (literature values range from 0.2 to 8.0 Å^2/molecule·min (7, 11, 25–27)) and not prone to domain growth resulting from diffusion-limited aggregation (28–30), the domains are nucleated in the form of bean-like shapes (from here on referred to as beans) and growth progresses from beans to shapes having an S-like appearance and finally culminates in multilobe shapes (showing three or four appendages). Examples of each of these shapes, taken under our microscope, are shown in Figs. 1a–1c. Florsheimer and Möhwald have proposed that the more complicated S-like and multilobe shapes are simply fused combinations of beans (11). While they make an excellent case for this mechanism, this proposal has not been substantiated by other researchers.

In this paper, we show that the behavior of DPPC monolayers is much more subtle than the general picture painted above. We show, for example, that the types and proportions of domain shapes are very sensitive to compression speed. Even more important, however, we find that if the monolayer is maintained in a state of two-phase coexistence for long times (over 12 h), then the DPPC domains all become nearly circular. Using the DPPC isotherm to estimate the fraction of LC phase that should be present at a given area, we also find an apparent violation of the lever rule, with less condensed phase observed than that predicted. This violation is not apparent when the film is aged and circular domains are formed. Finally, while fluorescence microscopy reveals that domains relax eventually (over many hours) to circular

shapes, the images show no obvious signs of perturbations or microstructural changes in the monolayer film. On the other hand, isotherms generated by compressing very slowly (0.19 Å^2/molecule · min), or those generated at quick speeds but only after the film was left stagnant for a few hours, are markedly different from isotherms produced if the film is compressed within an hour after it is spread. One likely explanation for this behavior is accumulation of impurities; we present evidence that these may be air-borne, and we use the measured variation in isotherms to estimate the level of possible contamination.

EXPERIMENTAL

L-α-1,2-Dipalmitoyl-sn-glycerophosphocholine (DPPC, >99%, Avanti Polar Lipids, Birmingham, AL) and 1-palmitoyl-2-[6[(7-nitro-2-1,3-benzoxadiazol-4-yl) amino]caproyl]-sn-glycero-3-phosphocholine (C6-NBD-DPPC, >99%, Avanti Polar Lipids) were used without further purification. Unless otherwise noted, chloroform (Fisher, HPLC grade) was used as a spreading solvent for all lipid solutions. Millipore water (18.3 MΩ-cm resistivity) was used as a subphase in isotherm measurements. All experiments were performed at 19.5°C.

Isothermal compressions ($\pi - A$ curves) of DPPC were performed on two different commercial film balances. The first was a film balance (KSV 5000, Finland) with a surface area of 707 cm^2. The film balance used for fluorescence microscopy experiments (R & K Ultrathin Organic Film Technology RK1, Germany) had a surface area of 144 cm^2. Both film balances were equipped with a Wilhelmy plate to monitor surface pressure. Although our balances read out to 0.01 mN/m, we estimate the sensitivity to be about 0.03 mN/m. We used plates made of either platinum or filter paper (with no significant differences noted between them). Monolayers were spread from lipid solutions in chloroform. Compression speeds and the time allowed before compression were varied as part of the analysis in this paper.

Video-enhanced fluorescence microscopy was conducted with the smaller balance placed on the stage of an epifluorescence microscope (Zeiss Axiotron, Germany). The film balance was enclosed in a Plexiglass housing and experiments were conducted in a Class-10,000 clean room. While the laboratory humidity was about 65%, the humidity within the enclosure was probably much greater. All fluorescence images were captured on a CCD camera (Quantex QC-200, Sunnyvale, CA) interfaced to a video monitor and a video cassette recorder. Image analysis and processing were done on taped images with commercial software (Presage, Advanced Imaging Concepts, Princeton, NJ). Monolayer imaging was carried out by doping the lipid solutions with 1 mol% C6-NBD-DPPC dye probe. The probe displays only liquid-expanded behavior, consistent with its partitioning into fluid monolayer phases (12, 31). Lipid fluorescence probes were excited using a 100-W OSRAM HBO W/2 Hg lamp.

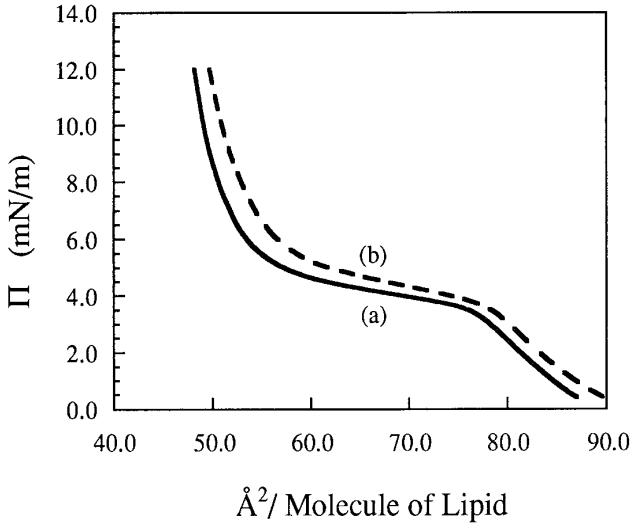

FIG. 2. $\pi - A$ isotherms for DPPC at 19.5°C: (a) compression speed of 2.57 Å^2/molecule min or 0.91 Å^2/molecule min; (b) compression speed of 0.19 Å^2/molecule min.

The microscope and film balance were placed on an antivibration isolation table (JRS, Switzerland). The Plexiglass enclosure reduces the influence of air currents, thus helping to abate unwanted domain travel as well as inhibiting subphase evaporation. Typically, barriers were allowed to compress the monolayer to the requisite surface pressure and then stopped. The video taping of domains was carried out when the barriers were at rest. This reduces (but does not stop) the convection of the water subphase and vibrations, which allows for better image quality. At times we also placed a glass filter in the bottom of the film balance to reduce the water depth and hence the water convection.

FEATURES OBSCURED: CHARACTERISTICS AND STABILITY OF OBSERVED DOMAIN SHAPES

The procedure generally followed to produce an isotherm of any given monolayer is to spread the film, wait for the spreading solvent to evaporate, and then compress the film at modest speeds, i.e., slow enough to avoid any known kinetic effects, but fast enough to make the experiment feasible and to dodge the many unwanted variables and problems that generally come into play as the time length of any experiment increases. This procedure for DPPC (allowing about a half-hour for the solvent to evaporate) yields identical isotherms (within experimental uncertainty $\approx$3 Å^2/molecule) for the two compression speeds of 2.57 and 0.91 Å^2/molecule · min. The resulting isotherm, at 19.5°C, is shown in Figure 2a, and agrees with the results of others reported in the literature (11, 26, 27). We note that at these two speeds, it requires about 30 and 85 min, respectively, to

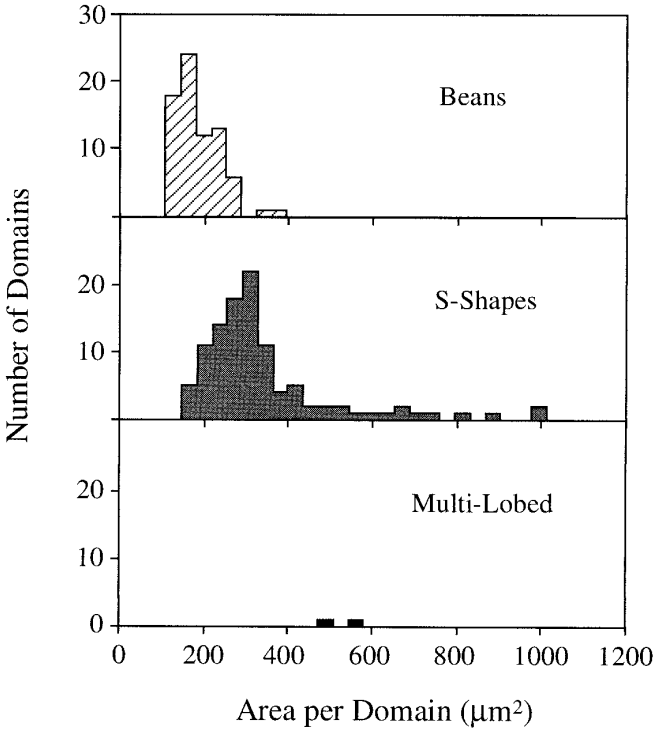

FIG. 3. Histogram of DPPC domain shapes for π = 4.1 mN/m, compressed at 0.91 Å^2/molecule min.

reduce the average area per molecule from 120 to 42 Å^2/molecule. In looking at the film under the fluorescence microscope it may also appear that the types, distribution, and progression of domain shapes formed in the LE/LC coexistence regime are similar for these two speeds, and follow the description provided in the Introduction (beans to S shapes to multilobed shapes). Quantitative image analysis reveals that they are not.

Before comparing the results for the two different speeds, we first note that at any given pressure in the two-phase regime, there can be significant amounts of different domain types (which we categorized as either beans, S shapes, or multilobed), and for each type, the range of areas can be large. In our analysis we hand sort domains into these three categories by inspection (this requires relatively few judgment calls); however, a commercial image analysis package is used to determine domain areas. Figure 3 shows the shapes and sizes of domains observed at π = 4.1 mN/m, reached by compressing the film at 0.91 Å^2/molecule · min (five separate experiments were used to generate statistics for these histograms). In accord with the qualitative description of domain evolution discussed in the Introduction, it is true that the mean area for a particular shape type increases as the pressure increases, as does the relative amount of higher order shape types (beans < S-like < multilobed). (This trend can be seen in Figs. 4 and 5, which are discussed next.)

For each compression rate, we generated a catalog of shape types and corresponding areas that were observed over a range of surface pressures from π = 3.7 mN/m to π = 4.3 mN/m (corresponding to decreases in molecular area from 73.0 to 64.6 Å^2/molecule) with data collected at increments of 0.1 mN/m. Five experiments were carried out at each compression speed to generate sufficient data. Note that one cannot use the resulting data set to determine the distribution of shapes at a particular pressure; rather this represents a composite picture of shapes observed over the range of pressures examined. The point is, however, that this composite profile is significantly different for the two compression speeds. At the faster rate there is a distinct lack of bean formation, as shown in Fig. 4; at the slower rate, only a minority of domains evolve to higher order shapes, with beans dominating the distribution as shown in Fig. 5.

Nag *et al.* have previously reported on the dependence of

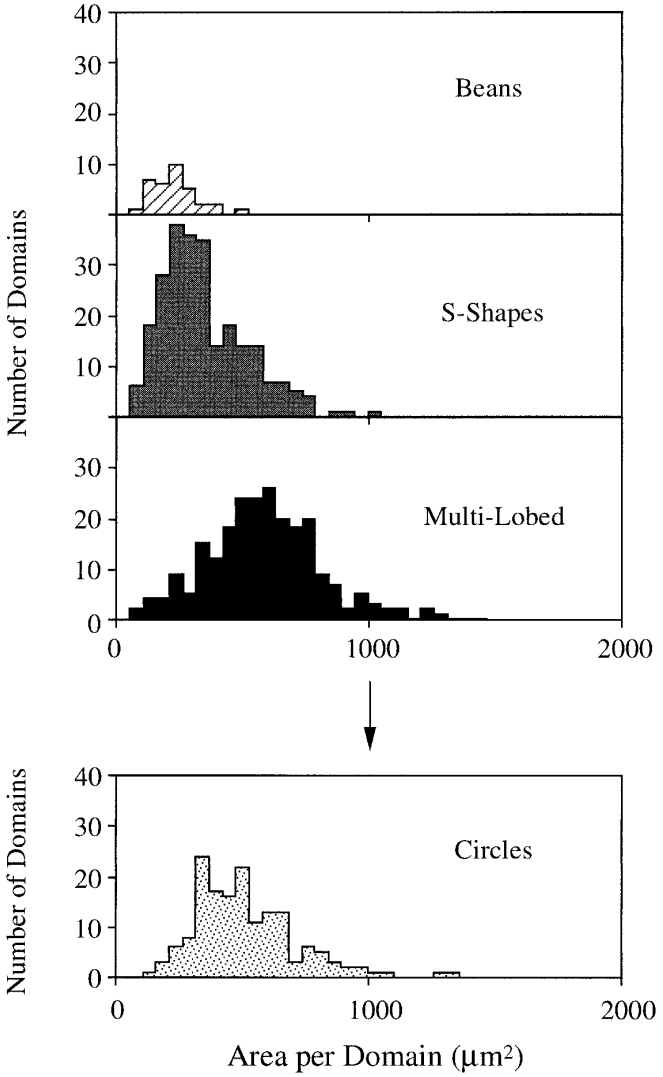

FIG. 4. Histogram of DPPC domain shapes (from π = 3.7 mN/m to π = 4.3 mN/m) compressed at 2.57 Å^2/molecule min.

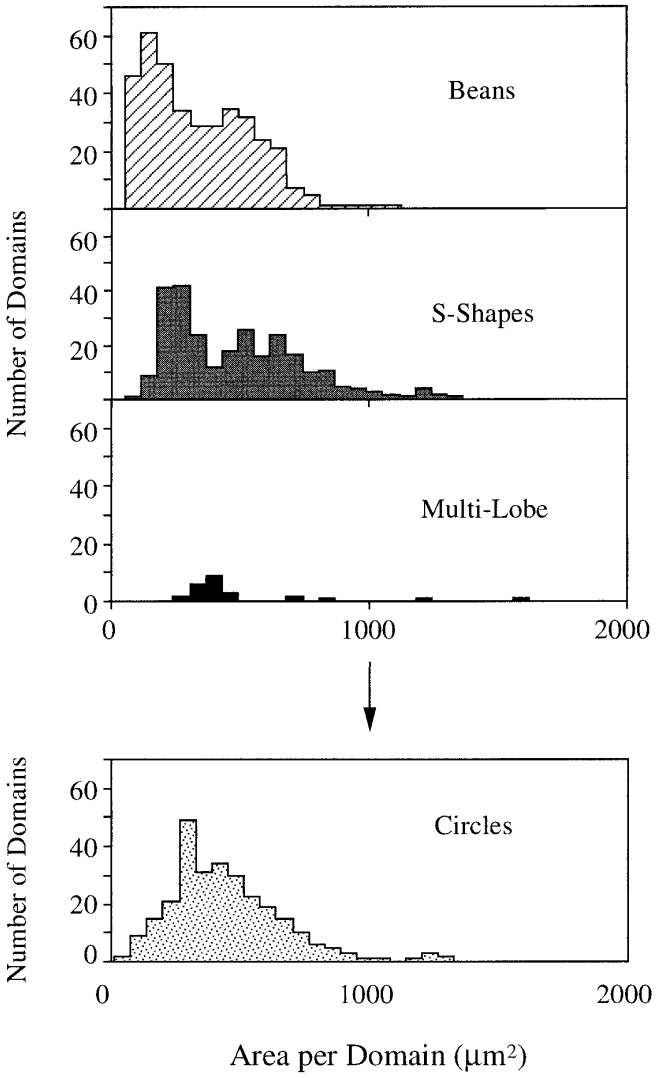

FIG. 5. Histogram of DPPC domain shapes (from π = 3.7 mN/m to π = 4.3 mN/m) compressed at 0.91 Å^2/molecule min.

domain size on compression speed, with faster compressions yielding smaller average domain sizes (25); however, they did not track any corresponding shape changes. Our data also support this finding, but in addition show that compression speed regulates the evolution of domain shapes. Of course at very fast compression speeds (nearing 60 Å^2/molecule·min), domains form dendritic shapes (28, 29) and speed directly controls domain morphologies. But the speeds studied here are much slower, and shapes observed appear stable over many minutes. (It is difficult to monitor a particular domain due to convection.) This has led some to postulate that beans (at smaller areas) and S-like shapes (at larger areas) represent the quasi-equilibrium morphologies (11, 25) of DPPC domains. Our compression rate studies clearly indicate that this is not the case.

Given that slower compression speeds favor the formation of beans, one might then conclude that this is the equilibrium shape of DPPC domains. To test this, we allowed a film exhibiting domains to age overnight (approx. 12 h). To our surprise, we found that all domains became nearly circular, as shown in Fig. 1d. Shown in the bottom of Figs. 4 and 5 are the resulting size distributions of the aged circular domains. The history of these two films (compressed at different rates) has little influence on the distribution of the aged domains: all are circular and have an average area of 521 μm^2 (in Fig. 4) and 491 μm^2 (in Fig. 5). Interestingly, the domains are not of uniform size, but have a dispersity of about 220 μm^2.

To the best of our knowledge, only one other group before us has made note of the formation of ''round'' DPPC domains. Yang and co-workers mention seeing such domains when they compressed a DPPC monolayer very slowly (at 2.0 Å^2/molecule·min) (26, 27). Inspection of their micrographs reveals, however, that their domains are far from the very regular, nearly circular shapes that we observe. On the other hand, theories of equilibrium domain shape, for both untilted (23) and tilted (24) film forming molecules, predict that multilobed shapes exist but are only metastable. Stable shapes are either circular (or nearly circular in the case of tilted molecules) or bilobed, the exact result depending on a system parameter which measures the relative strength of line tension to dipolar electrostatic forces acting within the film.

We also investigated the growth of domains formed not by compression at constant temperature but rather by cooling a monolayer at constant area. In these experiments a monolayer at 19.5°C was first compressed (at a rate of 0.91 Å^2/molecule·min) to a pressure of 4.1 mN/m (histograms of domain shapes observed at this particular pressure are, in fact, part of the data set used to generate Fig. 3). Next the monolayer was heated to 35°C, above the phase envelope, thus melting all the domains. After remaining at the elevated temperature for about an hour, the film was then cooled back to the original temperature of 19.5°C, at which point the surface pressure was again 4.1 mN/m. Two different cooling rates were examined. In the first case, the time required to cool the film was 30 min, and in the second case, 4 h; the corresponding distributions of shapes observed at the final pressure are shown in Figs. 6 and 7, respectively. Once again, we see a clear dependence on rate, with faster cooling producing more domains with shapes of higher order (Fig. 6). Notice too (Fig. 7) that even though domains are nucleated and grown over a range of elevated temperatures, beans (and only beans) persist after the 4-h cooling experiment. Hence much longer times are still needed for domains to relax to circular shapes.

It is perhaps not surprising to see evidence of some long time relaxation mechanisms in these phospholipid monolayers. The comprehensive and elucidating X-ray scattering studies of Schwartz *et al.* (32) on fatty acid monolayers

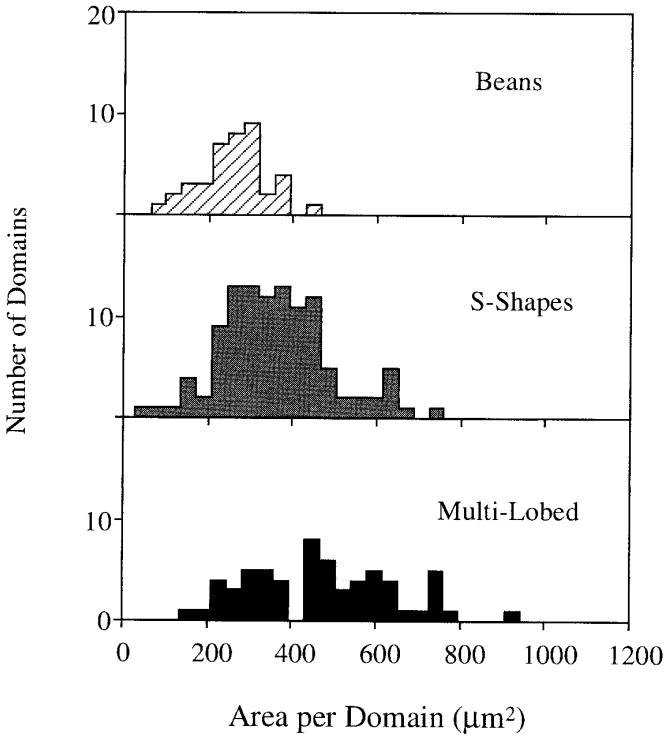

FIG. 6. Histogram of DPPC domain shapes for π = 4.1 mN/m formed by cooling over 30 min.

reveal that those systems relax from tilted to untilted phases over comparable times (many hours). It is not hard to imagine that very nonuniform molecular packing and ordering might underscore the characteristic yet complex shapes of DPPC domains shown in Fig. 1.

Further evidence that domain formation is a kinetically controlled process can be found by comparing the relative proportions of LE and LC phases actually observed to lever-rule predictions. Image analysis readily provides a measure of the fraction of condensed phase as a function of the film area. Interestingly, this relation is not very different for the two compression speeds we examined (even though the distributions and sizes of shapes are). Our results are also in excellent agreement with those reported by Nag *et al.* (25) and Florsheimer and Möhlwald (11). To compare experimental results with a lever-rule prediction, we assume that the mean molecular area of the liquid-expanded phase is 74.5 Å^2/molecule, corresponding to the area of the onset of the plateau, where a sharp kink in the isotherm is observed. We then find that to predict the observed amount of liquid-condensed phase, values for the LC mean molecular area must range from 50.2 Å^2/molecule (just after the onset of coexistence) down to 34 Å^2/molecule (at higher fractions of condensed phase). The latter value is considerably smaller than the molecular area determined by X-ray reflectivity (33), which is 46.0 Å^2/molecule (at π = 40.0 mN/m), or for that matter, smaller than the closed packed area for the two chains that compromise a DPPC molecule, which is about 40.0 Å^2/molecule (33). Although they may not have noticed it, apparent violations of the lever rule have also been seen in the work of other researchers. Both Nag *et al.* (25) and Florsheimer and Möhlwald (11) report that at 62 Å^2/molecule, the fraction of LC phase observed is 30%. To account for this fraction, the LC mean molecular area would be about 34.5 Å^2/molecule (obtained by using their isotherms to estimate the LE mean molecular area), which is in agreement with our findings.

We do not see this same phenomenon in films aged long enough to produce circular domain shapes. In this case, we find that the LC mean molecular area must equal 53.2 Å^2/molecule to predict the observed amount of LC phase. This is a larger area than that derived from X-ray reflectivity measurements. However, films probed in those measurements (33) were maintained at a surface pressure of π = 40.0 mN/m. Here, the surface pressure is much lower, and so a value of 53.2 Å^2/molecule seems reasonable, or least feasible, in light of the compressibility of the LC phase.

FEATURES REVEALED: SENSITIVITY OF ISOTHERMS TO EXPERIMENT DURATION

As documented in the previous section, we found that notably different domain shape distributions were produced at different compression speeds that otherwise yielded identical isotherms. We also found that DPPC films left idle for many hours in a state of two-phase coexistence displayed only circularly shaped domains. The latter observation motivated us to execute isotherms resulting from much slower compression rates (relative to those reported in the previous section) in an effort to capture the possible formation and growth of circular domains. We saw, as expected, that slower compression speeds favor the formation of lower order shapes (mainly beans); but even at the lowest speed examined (0.19 Å^2/molecule · min) we never saw the formation of shapes that would be classified as circular. What we did see, however, was a pronounced effect of experiment dura-

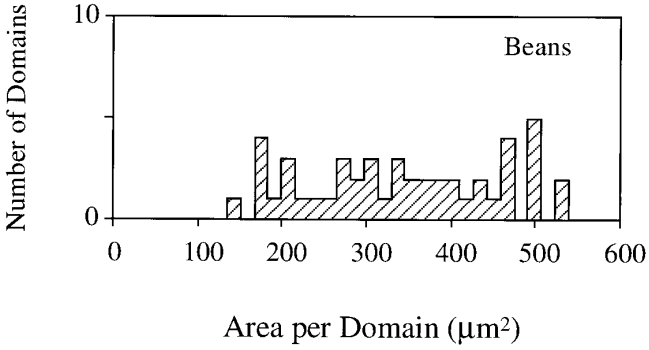

FIG. 7. Histogram of DPPC domain shapes for π = 4.1 mN/m formed by cooling over 4 h.

tion on the measured isotherms. For example, we found that the slower the compression speed (and therefore the longer the time required to complete the experiment), the more elevated the transition pressure corresponding to the onset of LE/LC phase coexistence and the steeper the isotherm in the two-phase regime. This behavior is illustrated in Fig. 2, which compares the isotherms generated at two compressions speeds: 2.57 and 0.19 $Å^2$/molecule · min, corresponding to total compression times of 30 min and 6.8 h, respectively.

Based on the results of the previous section, one might first wonder if the increase in surface pressure is related to the long time relaxation of the DPPC film. However, Schwartz *et al.*, who undertook painstaking measures in their X-ray studies to keep their fatty acid films clean, show that relaxation in these films is associated with a decrease in surface pressure and a flattening of plateaus (32).

Another possibility is that subphase evaporation accounts for the observed pressure increases. Indeed, the careful studies of Pethica and co-workers (34, 35) on *n*-hexadeconoic acid monolayers confirm that isotherms are affected by humidity; in particular, evaporation cools the surface and also changes the buoyant force acting on the Wilhelmy plate. Relative to isotherms produced at near 100% humidity, they found that those at 65% humidity exhibited a lower transition pressure (consistent with the ramifications of evaporation) and showed a slight increase in slope within the coexistence region (associated with retardation of evaporation with increasing film density) (35). While the latter effect is similar to what we observed, the former is not. So, although we did not explicitly control humidity (apart from housing the film balance in a Plexiglass enclosure), evaporation alone cannot fully account for the behavior of our isotherms.

A sufficient condition which leads directly to the observed variations in isotherms (i.e., an increase in transition pressure and increased slope in the coexistence region) is the presence of impurities (34–36). An isotherm can be considered a manifestation of the phase rule for a given system, and as such is extremely sensitive to changes in degrees of freedom. One of the most dramatic illustrations of this is the difference between two-phase equilibrium in single-component systems, which occurs at fixed pressure, and multicomponent systems, which occurs over a pressure range.

In the remainder of this paper, we elaborate on the experimental conditions which we found to affect the isotherms; all are in accord with the possibility that impurities, most probably air-borne, accumulate within the system. Therefore, we use colligative arguments, based on increases in transition pressure, to estimate the impurity level. Since it is well known that the introduction of a fluorescent probe (and thereby a second component) affects the isotherm in the same way as that described, we note that the experiments discussed from here on were carried out without the application of fluorescence microscopy and thus are free of probe. Since the first part of this paper reports on observations made using fluorescence microscopy, it is worth emphasizing the change in focus from those experiments to these that follow. The point of those experiments was to demonstrate the marked changes in domain shape that result from mechanical effects (namely variations in compression speed); the probe was maintained at fixed concentration throughout the study. Analysis and comparison of domain shapes were based on a simple classification scheme (beans, etc.) that neglects fine features which may indeed be influenced by the amount of probe present. On the other hand, we do believe that the overall classification scheme is useful, since similar domain types were seen in the AFM experiments of Yang and coworkers (26, 27), and also by us in our laboratory using Brewster angle microscopy.

Returning now to the isotherm experiments, one variable which notably influenced the measured isotherms was the amount of time the film was exposed to the environment. However, we also noticed that the surface pressure of the film during exposure played a role. For example, under similar laboratory conditions, different increases in transition pressure were observed for the following experiments, all having the same duration: (a) film allowed to wait for a given time in a fully expanded state (essentially $\pi = 0.0$ mN/m), and then compressed; (b) a film that was held at a $\pi = 12.0$ mN/m for the same period of time, then expanded, and then compressed; (c) a film that was continuously compressed but at much slower rates than those in (a) and (b).

To quantify the influence of surface pressure during exposure, it is useful to create a variable, $\hat{\pi}$, which represents the time-averaged pressure experienced by the monolayer over the course of the experiment:

$$\hat{\pi} = \frac{\int \pi(t)\,dt}{\int dt}.$$

All of our experiments had the same basic form: maintaining the monolayer at some constant pressure, π_{hold}, for some prescribed waiting time, t_{hold}, and a compression of the monolayer at some constant speed, dA/dt. In this case, the equation takes the form

$$\hat{\pi} = \frac{\pi_{\text{hold}} t_{\text{hold}} + (dA/dt)^{-1} \int_{A_1}^{A_2} \pi\,dA}{\text{Total time of experiment}},$$

where A_1 and A_2 are fixed limits for integration which we set to 110.0 and 50.0 $Å^2$/molecule, respectively.

To understand better the significance of $\hat{\pi}$, we note that any experiment that does not involve waiting has nearly the same $\hat{\pi}$; this is about 2.44 mN/m (in spite of the variations

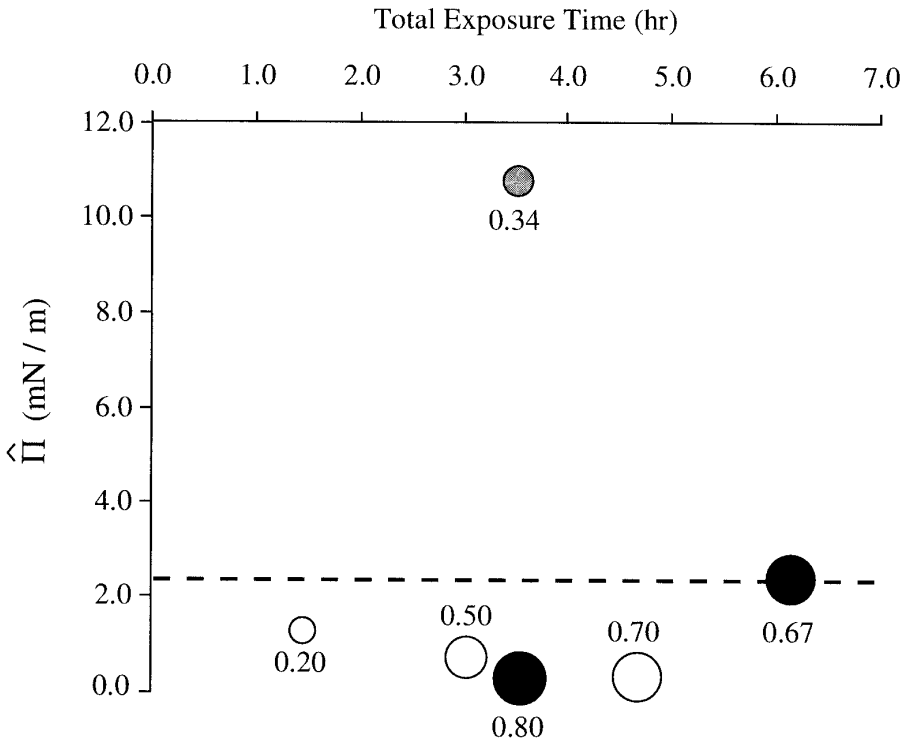

FIG. 8. Increase in transition pressure as a function of time-averaged pressure, $\hat{\pi}$, and total exposure time (the elapsed time from spreading to the end of compression). Areas of the symbols are scaled proportionally to reflect the magnitude of the surface pressure increase (as given by the numerical values). The dashed line corresponds to $\hat{\pi}$ for monolayers that are continuously compressed. Different types of symbols are used to distinguish the following situations: normal laboratory conditions (filled black circles); class 10,000 clean room conditions (open circles); a monolayer film held at π = 12.0 mN/m for 3 h under normal laboratory conditions (filled gray circle).

in isotherms that are produced for slower compression rates, as evidenced in Fig. 2). Experiments which involve holding the monolayer at any pressure lower (higher) than 2.44 mN/m will have a smaller (larger) $\hat{\pi}$. As an illustration, consider the resulting values of $\hat{\pi}$ for three experiments similar to those discussed above: (a) film held 3 h at π = 0.0 mN/m before being compressed at a rate of 2.57 Å^2/molecule · min, $\hat{\pi}$ = 0.35 mN/m; (b) film held 3 h at π = 12.0 mN/m, then rapidly expanded, and then compressed at a rate of 2.57 Å^2/molecule · min, $\hat{\pi}$ = 11.1 mN/m; (c) film continuously compressed, $\hat{\pi}$ = 2.44 mN/m.

We thus use two variables to characterize the history of a film during an experiment: $\hat{\pi}$ and total exposure time. As a function of these variables, we plot in Fig. 8 points which represent the increase in transition pressure above that for the reference isotherm shown in Fig. 2a; areas of the symbols are scaled in proportion to reflect the magnitude of this increase. Three trends emerge to provide evidence that impurities account for the noted changes in isotherms. First, by examining the open symbol data in Fig. 8, it can seen that for the same laboratory conditions (class 10,000 clean room) the transition pressure increases as t_{hold} increases; in this case the monolayers were compressed at the same rate after being held at $\hat{\pi}$ = 0.0 mN/m for 1.5, 3.0, and 4.5 h. Second, for the same film variables (i.e., same approximate $\hat{\pi}$ and total exposure time), different laboratory conditions produce different increases in transition pressure. Compare the two nearest open and closed symbols in Fig. 8, corresponding to experiments performed in a clean room and under normal laboratory conditions, respectively. As expected, the latter demonstrates a larger increase in transition pressure. Finally, we note that films held for equal times at different surface pressures do not display the same increase in transition pressure. Films characterized by a higher $\hat{\pi}$, and thus a lower surface energy, experience less of an increase (see, for example, the gray circle, which corresponds to a film held at π = 12). In other words, more impurities adsorb to higher energy surfaces.

We used a simple colligative argument to estimate the amount of impurities that would cause our measured increases in transition pressure. We assume that a DPPC film contains a small amount of a second component, namely the impurity, which is insoluble in the LC phase. Equivalence of the chemical potential of the DPPC in both phases then leads to the following relation for the mole fraction of impurity in the film:

$$x_I = \left[\frac{(A_{LC} - A_{LE})}{RT}\right]\Delta\pi.$$

Here $\Delta\pi$ is the increase in transition pressure relative to that for pure DPPC, A is the molecular area of DPPC in the given phase, and RT is the thermal energy. The coefficient in brackets is about 0.087 m/mN for our experiments, so numbers reported in Fig. 8 (which are $\Delta\pi$) can be readily converted to estimates of impurity content.

Using this relation we find that our films contain impurities up to levels as high as 7%. This is higher than values predicted by other researchers. Although the purity of samples as received is claimed to be better than 99%, Pethica and co-workers (34, 30) have shown that careful and exhaustive purification procedures can increase this to greater than 99.9%. Smaby and Brockman (37) (using a surface potential analysis) report estimates of impurities as high as 1% in their particular monolayer films. However, their films were not aged for the same extended length of time as ours, so we believe that our estimates are physically realizable. To establish a reasonable upper bound for impurity content, we intentionally corrupted a monolayer film by exposing it to heptane during a compression. This was done by isolating the film balance in a Plexiglass enclosure that also contained saturated heptane towels as well as beakers filled with heptane. After a half-hour equilibration, the film was then compressed. As expected, this film demonstrated the largest increase in transition pressure as well as a dramatic increase in slope throughout the coexistence region. Using the relation above, the concentration of heptane was estimated at 13%.

We made some attempt to establish the origin and nature of suspected impurities. One of the likeliest sources is the spreading solvent, e.g., impurities in it, or remnants of it. We varied our spreading solvent from chloroform to a hexane/ethanol mix, but this had no affect on impurity levels. We even eliminated spreading solvent all together. For this, we sprinkled DPPC crystals on the surface of our film balance and allowed the film to equilibrate for 2 h. After this time, the surface pressure leveled off at approximately 0.04 mN/m, a very small value and just within the sensitivity of our Wilhelmy plate balance. Upon compression, we found that this film displayed an isotherm similar to one that had been formed using a spreading solution and allowed to wait for the same period of time before compression.

We also carried out similar studies for another monolayer, dipalmitoylphosphatidylethanolamine (DMPE), and found that similar film conditions led to similar estimates of accumulated impurities; so the effect observed is not specific to DPPC. Finally, we spread films on aged subphases, in particular water that was left stagnant for 24 h. Isotherms produced on this subphase were similar to isotherms produced on a freshly prepared subphase. Hence we speculate that air-borne molecules are the main source of impurities.[2]

We did not pursue any further attempts to characterize the composition of our films. However, we do note that our fluorescence microscopy observations of films maintained in two-phase coexistence for up to a day show no indication of dust or foreign matter. On the contrary, only very regularly shaped circular domains are observed. Clearly in this case fluorescence microscopy images give no indication that something has happened to the film, but instead leaves the experimenter with a false sense of security.

[2] One possible source, as pointed out by a referee, is the Plexiglass box.

CONCLUSION

The structure and phase behavior of water-supported monolayers are not a new area of research; rather it has been a focus of attention in many laboratories at various times since the pioneering work of Irving Langmuir over 75 years ago. Furthermore, although a variety of different film forming molecules have been investigated during this span, the lion's share of effort has been directed at a handful of systems, which include fatty acids and phospholipids. One might therefore be tempted to believe that such systems are well understood. On the contrary, we are still at the stage where application of new or more powerful techniques (most notably synchotron X-ray scattering) yields significant new information that often tears apart the current understanding. Additional information and insights can also be reaped from routine experiments, just by paying closer attention. This work is a case in point.

Although DPPC forms liquid-condensed domains with very characteristic shapes (beans, S-like, or multilobed), we have shown that the distribution of shapes is very sensitive to the rate of solidification. Slower rates—obtained either by a slower rate of compression at fixed temperature or by a slower rate of cooling at fixed area—yield distributions weighted more heavily with bean-like shapes. This clearly suggests that the monolayer is not in an equilibrium state. Analysis of domain areas (irrespective of domain shapes) as a function of degree of solidification also supports this, since violations of the lever rule are apparent. There appear to be relaxation mechanisms operative over very long time scales since monolayers allowed to relax for up to 12 h display domains that are nearly circular in shape. Conceivably such shapes represent the most stable morphology, although we observed a significant spread in their sizes.

Finally, our investigations also emphasize the importance of cleanliness, purity, and environmental control in studies of monolayers. We noted marked changes in measured isotherms as a function of experiment duration. Our best explanation for this is the accumulation of air-borne impurities. Given the long relaxation times that may be operative, experiments directed at probing the equilibrium properties of pure films will require scrupulous preparation and painstaking environmental regulation.

ACKNOWLEDGMENTS

We gratefully acknowledge the support for this work provided by the National Science Foundation Presidential Young Investigator Program (Grant CTS-89-57051) and the David and Lucile Packard Foundation.

REFERENCES

1. Stallberg-Stenhagen, S., and Stenhagen, E., *Nature* **156,** 239 (1945).
2. Bibo, A. M., and Peterson, I. R., *Adv. Mater.* **2,** 309 (1990).
3. Schwartz, D. K., and Knobler, C. M., *J. Phys. Chem.* **97,** 8849 (1993).
4. Durbin, M. K., Malik, A., Ghaskadvi, R., Shih, M. C., Zschack, P., and Dutta, P., *J. Phys. Chem.* **98,** 1753 (1994).
5. Overbeck, G. A., and Mobius, D., *J. Phys. Chem.* **97,** 7999 (1993).
6. Von Tscharner, V., and McConnell, H. M., *J. Biophys.* **36,** 409 (1981).
7. Lösche, M., Sackman, E., and Möhwald, H., *Ber. Bunsenges. Phys. Chem.* **87,** 848 (1983).
8. Stine, K. J., and Knobler, C. M., *Ultramicroscopy* **47,** 23 (1992).
9. Mao, G., Tsao, Y., Tirrell, M., Davis, H. T., Hessel, V., van Esch, J., and Ringsdorf, H., *Langmuir* **10,** 4174 (1994).
10. Weiss, R. M., and McConnell, H. M., *Nature* **310,** 47 (1984).
11. Florsheimer, M., and Möhwald, H., *Chem. Phys. Lipids* **49,** 231 (1989).
12. McConnell, H. M., Tamm, L. K., and Weiss, R. M., *Proc. Natl. Acad. Sci.* **81,** 3249 (1984).
13. Henon, S., and Meunier, J., *Rev. Sci. Instrum.* **62,** 936 (1991).
14. Hönig, D., and Möbius, D., *Thin Solid Films* **210/211,** 64 (1992).
15. Henon, S., and Meunier, J., *J. Chem. Phys.* **98,** 9148 (1993).
16. Overbeck, G. A., Hönig, D., Wolthaus, L., Gnabe, M., and Möbius, D., *Thin Solid Films* **242,** 26 (1994).
17. Keller, D. J., Korb, J. P., and McConnell, H. M., *J. Phys. Chem.* **91,** 6417 (1987).
18. McConnell, H. M., and Moy, V. T., *J. Phys. Chem.* **92,** 4520 (1988).
19. Andelman, D., Brochard, F., and Joanny, J. F., *J. Chem. Phys.* **86,** 3672 (1987).
20. McConnell, H. M., and de Koker, R. J., *J. Phys. Chem.* **96,** 7101 (1991).
21. Mayer, M. A., and Vanderlick, T. K., *Langmuir* **8,** 3131 (1992).
22. Langer, S. A., Goldstein, R. E., and Jackson, D. P., *Phys. Rev. A* **46,** 4894 (1992).
23. Mayer, M. A., and Vanderlick, T. K., *J. Chem. Phys.* **100,** 8399 (1994).
24. Mayer, M. A., and Vanderlick, T. K., *J. Chem. Phys.* **103,** 9788 (1995).
25. Nag, K., Boland, C., Rich, N., and Keogh, K. M. L., *Biochim. Biophys. Acta* **1068,** 157 (1991).
26. Yang, X. M., Xiao, D., Xiao, S. J., and Wei, Y., *Appl. Phys. A* **59,** 139 (1994).
27. Yang, X. M., Xiao, D., Xiao, S. J., Lu, Z. H., and Wei, Y., *Phys. Lett. A* **197,** 195 (1994).
28. Miller, A., Knoll, W., and Möhwald, H., *Phys. Rev. Lett.* **56,** 2633 (1986).
29. Miller, A., and Möhwald, H., *J. Chem. Phys.* **86,** 4258 (1987).
30. Helm, C. A., and Möhwald, H., *J. Phys. Chem.* **92,** 1262 (1988).
31. Lösche, M., and Möhwald, H., *Rev. Sci. Instrum.* **55,** 1968 (1984).
32. Schwartz, D. K., Schlossman, M. L., and Pershan, P. S., *J. Chem. Phys.* **96,** 2356 (1992).
33. Helm, C. A., Möhwald, H., Kjaer, K., and Als-Nielsen, J., *Europhys. Lett.* **4,** 697 (1987).
34. Middelton, S. R., Iwahashi, M., Pallas, N. R., and Pethica, B. A., *Proc. R. Soc. London Ser. A* **396,** 143 (1984).
35. Pallas, N. R., and Pethica, B. A., *Langmuir* **1,** 509 (1985).
36. Lösche, M., and Möhwald, H., *Eur. Biophys. J.* **11,** 35 (1984).
37. Smaby, J. M., and Brockman, H. L., *Chem. Phys. Lipids* **58,** 249 (1991).